

EXPERIMENTAL AND ANALYTICAL INVESTIGATIONS ON FLEXURAL PERFORMANCE OF CORRODED RC BEAMS USING RBSM-BASED CORROSION MODEL

Nguyen Cong Luyen^{1*}, Mai Anh Duc¹, Nguyen Hong An²

¹The University of Danang - University of Science and Technology, Vietnam

²Ho Chi Minh City University of Technology, Vietnam

*Corresponding author: ncluyen@dut.udn.vn

(Received: February 26, 2024; Revised: March 22, 2024; Accepted: April 22, 2024)

Abstract - Residual strength and structural performance of reinforced concrete (RC) structures subjected to rebar corrosion need to be precisely evaluated for an efficient rehabilitation process. However, the performance of deteriorated structures cannot be specified by using design methods since the damaged conditions are different in each type of structures due to corrosion degree, corrosion position, environmental condition. This study first presents an experimental investigation on the flexural performance of RC beam subjected to rebar corrosion. To complement the test data, an analytical corrosion model developed by the authors, which is based on Rigid Body Spring Method (RBSM), was employed. The results obtained from both analytical model and experiment confirmed that the corroded beam appeared to obtain a significantly lower bending stiffness and lower flexural capacity than those of the sound beam. The developed corrosion model can be able to capture the load-displacement curve of experimental results with good agreement.

Key words – Flexural performance; Rigid Body Spring Method (RBSM); Rebar corrosion; Bending stiffness; Analytical model

1. Introduction

Many reinforced concrete (RC) structures have been built for several decades all over the globe, and most of these aging infrastructures have become damaged by various factors in their service life, such as rebar corrosion, carbonation, and alkali-aggregate reaction. Among the above-mentioned factors, rebar corrosion is one of the most critical consequences of aging RC members subjected to chloride ingress and carbonation [1]. Naturally, the alkalinity of concrete is high, forms the passive film around the rebar, and protects the rebar from corrosion. However, when chloride ion penetrates into concrete, it can destroy the film directly, which then triggers rebar corrosion, resulting in the loss of rebar diameter and expansion cracking causing the degradation of structural performance. For this reason, deterioration due to rebar corrosion can threaten the structural performance and pose a risk to human lives [2-4].

To efficiently rehabilitate corrosion-damaged RC structures, damage progress and residual strength of the deteriorated structures must be determined and investigated. However, the performance of deteriorated structures cannot be specified by design methods since the damaged conditions are different in each type of structures due to corrosion degree, corrosion position, environmental condition. To address these drawbacks, few researchers conducted experimental programs to investigate the structural performance of corroded RC structures. For

instance, Carlo et al. [5] experimentally investigated the flexural behaviour of corroded RC beams under bending load subjected to different corrosion rates. However, experimental programs seem to be expensive and time-consuming to investigate the structural performance of corroded RC structures. Thus, there is an urgent need to develop numerical/analytical tools that can effectively evaluate and predict the corrosion-induced crack propagation and residual strength of corroded RC structures. For this purpose, few studies have been reported in literature. Toongoenthong and Maekawa [6] developed a numerical model using the finite element method (FEM), which is composed of three types of elements, i.e. expansive material element, plain concrete element and interface element. Tran et al. [7], by using a three-dimensional Rigid-Body-Spring-Method (RBSM), proposed a three-phase material corrosion expansion model including rebar, corrosion products and concrete. Ozbolt et al. [8] built a 3D chemo-hydro-thermo-mechanical FEM model which also consisted of three layers: a concrete part, a rust layer, and a reinforcement part. The above-mentioned models acquire merits that 3D modeling of rebar is assumed and corrosion expansion pressure is introduced directly in the corrosion product layer around the rebar. Therefore, these models can be able to simulate corrosion-induced cracking behavior in concrete specimen. However, in such models, solid element is employed to model the rebar which is somewhat computationally expensive. On the other hand, in structural analysis, rebar is normally modeled by beam element, which assists the modeling process in structural level to be faster. Thus, using 3D-modelling rebar models like the above-mentioned approaches are almost unlikely to simulate corrosion analysis combined with structural analysis. Other studies [9] analyzed the flexural performance of corroded RC beams by using ABAQUS program. Beam element was used for the rebar. Nevertheless, the corrosion modeling process was not considered in this model. Therefore, a model that can reasonably simulate both corrosion-induced cracking behavior and structural behavior with corrosion damages of RC member would be essentially needed. Recently, the author has successfully developed a model that employed beam elements for simulating the rebar in which rebar corrosion is modeled using corrosion expansion area [10, 11]. The developed model was then validated against experiment using specimens with single rebar and different

cover thickness, different rebar's diameter, different specimens' size. The relationship between surface crack width and corrosion amount was clarified and the results showed good agreement between the model and test [10]. The model was also used to simulate the effect of multi-rebar arrangement on the shape and opening of surface and internal cracks [11]. The influence of rebar corrosion on bond behaviour of damaged RC structures was also clarified in the previous research [11]. In this study, the developed corrosion model is used to investigate the flexural behaviour of RC members subjected to rebar corrosion. The results obtained from the model will be compared with test results conducted by the authors. Further discussion on flexural behaviour of corroded RC structures is provided.

2. Developed analytical model

2.1. Three-dimensional RBSM

In the analysis, three-dimensional RBSM was employed [12]. The RBSM as a discrete numerical approach represents a continuum material as an assemblage of rigid particles interconnected by zero-length springs along their boundaries as indicated in Figure 1. The particle elements are randomly generated with Voronoi diagram. Each of the elements has six degrees of freedom at its nucleus. Three springs, one normal and two shear springs, are defined at the center point of each triangle formed by the center of gravity and the vertices of the boundary between two elements. Nonlinear material models of concrete were introduced into the springs. The response of the spring model provides an understanding of the interaction between particles instead of the internal behavior of each element based on continuum mechanics [12].

2.2. Modeling of reinforcement and corrosion expansion area

2.2.1. Modeling of reinforcement by beam element

Figure 2 shows the reinforcement model, which is formed as a series of regular beam elements. In this model, the reinforcement can be freely positioned within the members, regardless of the mesh size of the concrete [12].

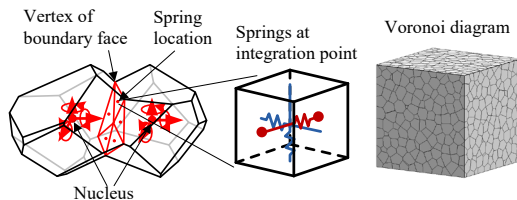


Figure 1. Three-dimensional RBSM

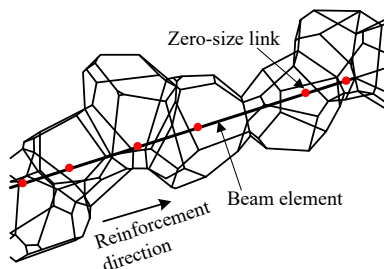


Figure 2. Reinforcement arrangement

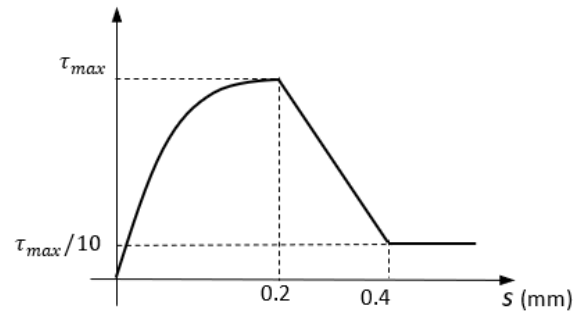


Figure 3. Bond stress-slip relationship

At the beam node, two translational and one rotational degree of freedom are defined by mechanical springs. The reinforcement is attached to the concrete particles by zero-size link elements that provide a load-transfer mechanism between beam node and the concrete particles [12].

The stress-strain relation of reinforcement is defined by a bilinear model. Crack development is strongly affected by the bond interaction between concrete and reinforcement. The bond stress-slip relation is provided in the spring parallel to the reinforcement of link element. Figure 3 shows the relation that is defined by Eq. (1) up to peak strength [13] and the curve proposed by CEB-FIB is assumed after peak strength:

$$\tau = 0,36 f_c^{2/3} \{1 - \exp[-40(s/D)^{0.5}]\} \quad (1)$$

where D is diameter of the reinforcement and s represents the slippage.

2.2.2. Modeling of corrosion expansion area

To simulate corrosion-induced crack propagation, modeling of real rebar's parameters such as diameter and surface are obviously important since the cracking pattern and surface crack width are strongly influenced by the ratio of cover thickness and rebar diameter as well as local corrosion area around the rebar. However, as beam element which is used for modeling of rebar does not have a real area like solid element, the authors thus propose the virtual expansion area which is the same as the cross-sectional area of the rebar (Figure 4) [10, 11]. In such an area of concrete, initial strain is set in normal spring which is located on boundary surfaces between Voronoi elements. Initial strain is calculated based on expansion pressure U which depends on corrosion amount [7]:

$$U = \frac{W_r (\alpha_{cor} - 1)}{\rho_s} \quad (2)$$

where, α_{cor} is the volume-expansion ratio of corrosion products, assumed 2.5 in this study. ρ_s is rebar density ($7.85 \times 10^3 \text{ mg/cm}^3$), W_r is corrosion amount (mg/cm^2), calculated by:

$$W_r = \frac{\rho_s V_{loss}}{2\pi r L} \quad (3)$$

where, V_{loss} is the volume of steel loss (cm^3), L is the rebar length, r is the rebar radius.

Due to the use of elastic modulus of concrete instead of that of corrosion products in real structure for calculating corrosion expansion stress, the stress of concrete in the model

would increase faster than that in real structure. Moreover, due to the difference between real area of rebar in real structure and virtual area of rebar in the model, U is modified by multiplying with modification factor β of 0.3 [10]:

$$U_{md} = U \cdot \beta \tag{4}$$

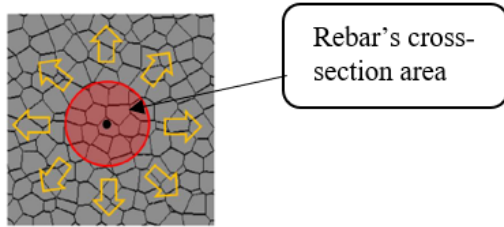


Figure 4. Corrosion expansion model

2.3. Modeling of local corrosion around the rebar

It has been known that the chloride ion diffusivity through cracked concrete is much more than through uncracked concrete. In this study, HALF corrosion model will be applied in a way that only half of the rebar surface area is given an incremental expansion strain, as shown in Figure 5b. Several assumptions are applied when taking into account this effect:

- Rebar is locally corroded when a vertical crack above the rebar exceeds 0.2 mm in width.
- Increment of initial strain in Eq. (4) is only applied over the half virtual area of rebar's cross-section.
- The total corrosion product amount in local corrosion model is similar to that in uniform corrosion model (Figure 5a) at the same corrosion amount.

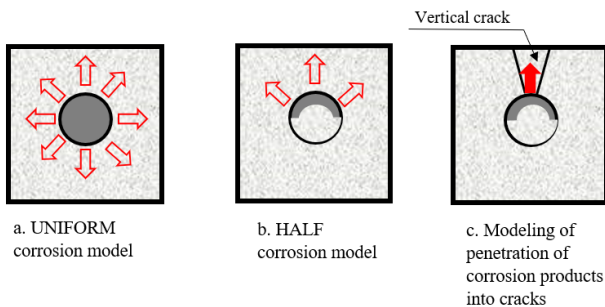


Figure 5. Modeling of the effects of local corrosion and penetration of corrosion products

3. Experimental study

3.1. Specimen outline and material properties

Test program was conducted to investigate the effect of rebar corrosion on flexural behaviour of RC beam. Specimen dimension and reinforcement arrangement are shown in Figure 6. Specimen has cross-section 150 mm x 150 mm and 1800 mm in length, which was arranged with one rebar D13 hooked on both ends to prevent anchored failure.

In order to investigate the effect of rebar corrosion on flexural behaviour, two beams were cast: a sound beam (Figure 6a) and a corrosion beam which was only corroded in 1400 mm middle span with corrosion target 10%, named as B1400-10%, as illustrated in Figure 6b.

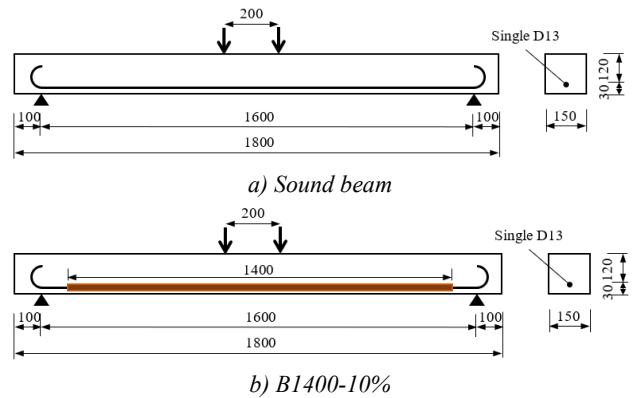


Figure 6. Specimen outline

The concrete compressive strength and elastic modulus of sound beam at the time of testing were 37 MPa and 30 GPa, respectively, for corroded beam were 30 MPa and 28 GPa, respectively. The differences in concrete compression strength and elastic modulus between sound and corroded beams do not affect their theoretical flexural capacity and initial stiffness, with deviation between them only 1.7% for flexural capacity and 2.3% for initial stiffness.

3.2. Corrosion test

The B1400-10% was subjected to an accelerated electric corrosion test with a target corrosion rate of 10% calculated by Faraday law. Upon finishing loading test, the corroded bar was taken out and immersed in a 10% ammonium hydrogen citrate solution for 24 hours to cleaning. The rebar was then cut into several small parts with 50 mm in length to measure corrosion rate distributed along the beam. Figures 7 and 8 show that corrosion degree and mass loss varied along the beam, indicating that a high corroded rate can be seen at the middle parts and a low corrosion rate is distributed in other areas. The average corrosion degree in this beam is considered to be approximately 10%.

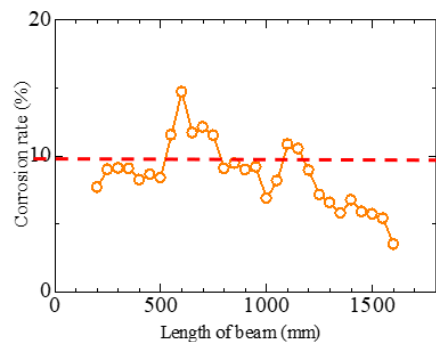


Figure 7. Corrosion rate distributed along the beam

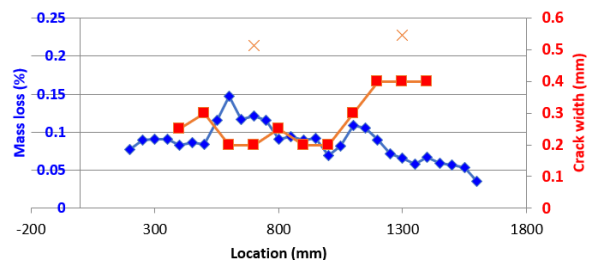


Figure 8. Crack width and rebar's mass loss along the beam

3.3. Test setup and results

After finishing corrosion test, the beams were then loaded under four-point loading, as shown in Figure 9. Crack gauges were arranged at the middle of the beam to measure the crack width (Figure 10). For the instrumentation plan of the tests, three linear variable displacement transducers (LVDTs) were installed at the bottom of the HSS section at the mid-span (LVDT-1) and at the loading points (LVDT-2 and 3) (Figure 9). All the beams were tested under displacement control at a rate of 0.5 mm/min until the beam was yielded. The loading rate was then increased to 1 mm/min and kept continuing until a mid-span deflection of approximate 40 mm was reached. During the test, data were recorded once every 10s by the automatic data logger system. Load–displacement relationship and crack pattern at failure of sound beam and B1400-10% beam are plotted in Figures 11 and 12.



Figure 9. Test set-up



Figure 10. Crack gauges at the middle of the beam

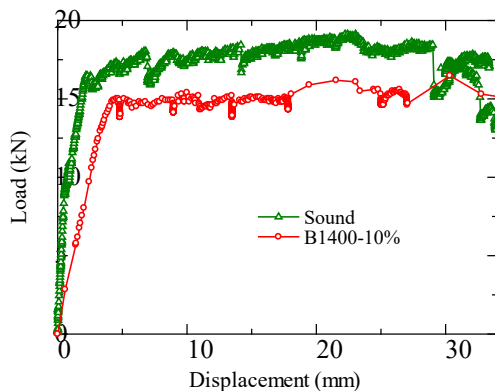


Figure 11. Load – displacement relationship in sound and corroded B1400-10% beams

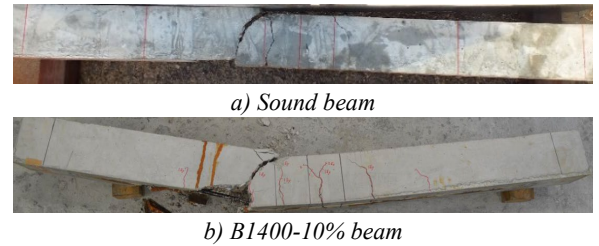


Figure 12. Crack pattern at failure

It has been shown that both beams failed in flexure and sound beam appears to obtain higher flexural capacity and higher bending stiffness than those of corroded beams. As mentioned earlier, this significant difference should not be accounted for the difference in mechanical properties, which is only 1.7% for flexural capacity and 2.3% for initial stiffness. It seems that due to corrosion, bond strength in corroded B1400-10% beam was decreased. This effect combined with bond crack and reduction of rebar's area due to corrosion resulted in the significant degradation in bending stiffness and flexural strength.

4. Analytical modeling and results

Analytical model using RBSM that has been developed in [8, 9] is shown in Figure 13. Mesh size in area near rebar was made with 10 mm and 30 mm for other areas. Before load was applied, corroded B1400-10% beam was subjected to corrosion analysis with a target corrosion rate of 10%. The cracks due to corrosion in this beam are indicated in Figure 14. It is noted that as corrosion was only applied for 1400 mm in the middle of rebar's length, corrosion cracks were occurred only in these parts.

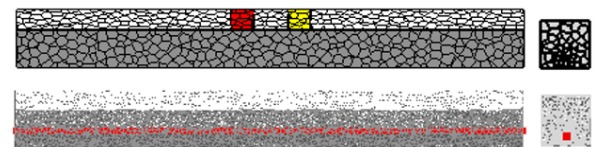
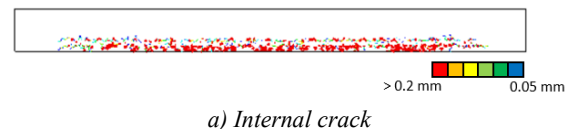


Figure 13. Analytical RBSM model



a) Internal crack



b) Surface crack (magnification: 5)

Figure 14. Corrosion crack in B1400-10% beam

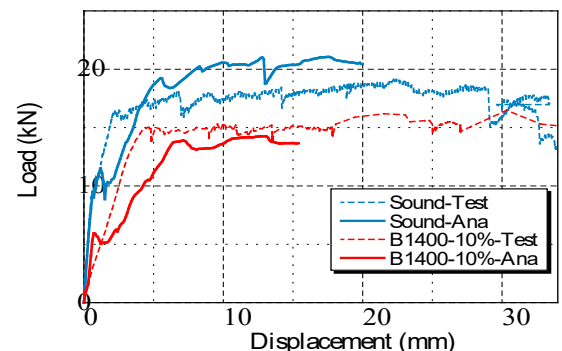
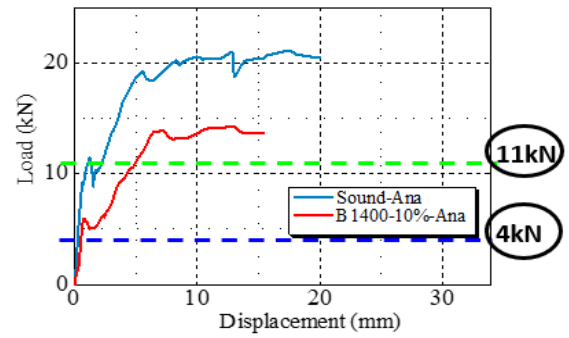
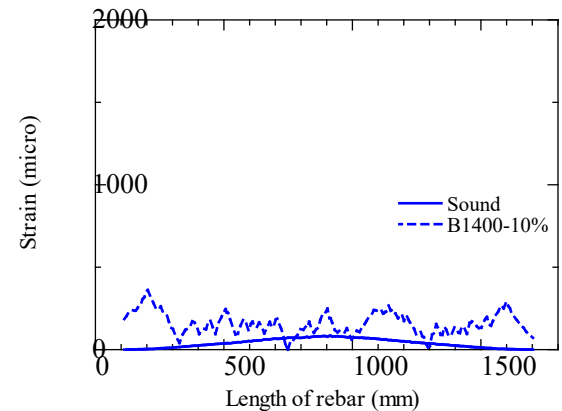


Figure 15. Load – displacement relationship obtaining from analysis in comparison to experiment

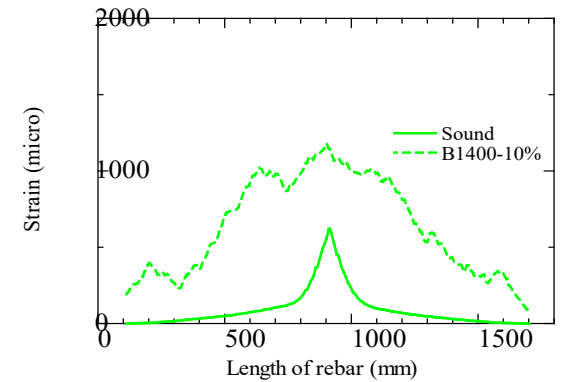
Figure 15 shows the load–displacement relationship curves obtaining from analytical model versus experiment. In sound beam, despite having a bit higher in flexural capacity, analytical results show a good correlation with test in terms of stiffness and failure mode. Pre-cracked load of analytical model almost coincides with experiment. When a crack occurred, the load was reduced slightly and then increased again until the beam reaches its flexural capacity. On the other hand, in corroded B1400-10% beam, when the load is still low, the load – displacement curve shows almost no difference with that of sound beam. Thereafter, when the first flexural crack occurred, the load was decreased and then increased again; however, it could not reach the same stiffness as before and finally failed at the earlier flexural load. Figure 16 exhibits that crack patterns at failure of both beams obtained by the analytical corrosion model are similar to test results.



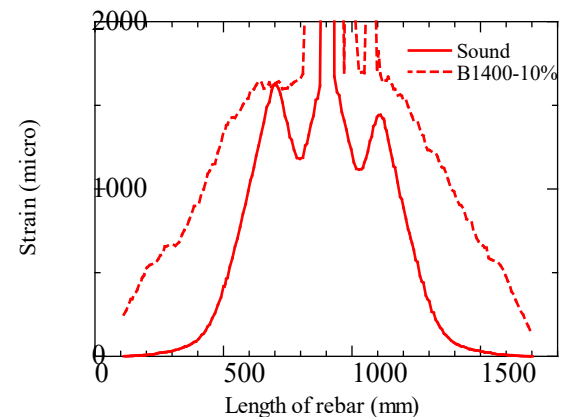
a) Load – displacement curve obtained from analysis



b) at 4kN



c) at 11kN



d) at peak load

Figure 17. Strain distributed along the rebar at several loading levels

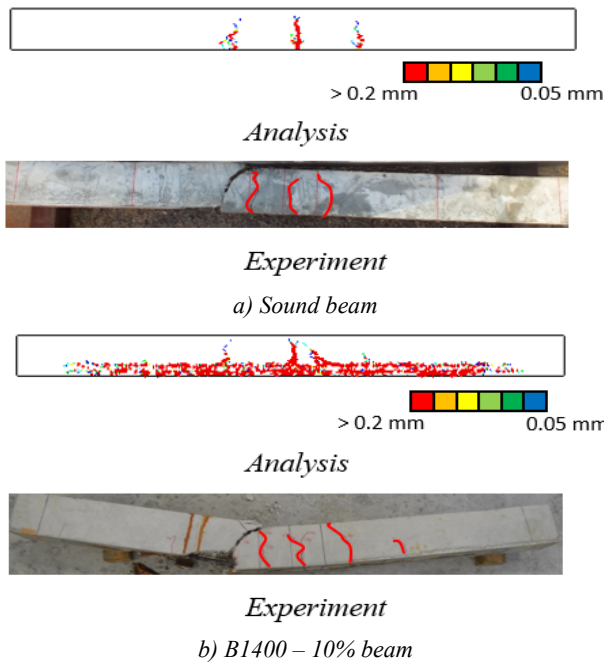


Figure 16. Crack pattern at failure

Figure 17 shows a piece of evidence that high strain value is distributed along the rebar at every typical loading stage. It is indicated that at the load of 4 kN and 11 kN, while strain in sound beam distributes linearly, strain in corroded rebar in beam B1400-10% appears unstable tendency, which has proved that due to bond strength reduction, stress in rebar could not be transferred to concrete and causes high strain in rebar. This result once again confirmed with experimental result that due to the reduction of bond strength combined with corrosion crack and reduction of rebar’s area, beam’s bending stiffness was decreased and consequently the beam failed at early flexural strength. At peak load (Figure 17d), rebars in both beams are yielded, meaning that flexural failure occurs in these two beams. In all these stages, rebar’s strain in beam B1400-10% was always significantly higher than that in sound beam.

5. Conclusions

The flexural behaviour of RC beam with corroded rebar has been investigated experimentally and analytically in this paper. Key conclusions can be drawn from this study:

(1) The experimental results showed that corroded beam appeared to have significantly lower bending stiffness and lower flexural capacity than those of sound beam.

(2) RBSM-based corrosion model agreed well with the experimental results not only in terms of bending stiffness but also the flexural capacity of the beam as well as the crack patterns at failure stage.

(3) Strain distribution evidence obtained from the RBSM-based corrosion model exhibited that corrosion crack occurred along the rebar caused difficulty in transferring the stress from rebar to concrete, resulting in the high strain in corroded rebar compared to that in sound beam. This effect in conjunction with corrosion crack and reduction of rebar's area explains for the significant degradation of bending stiffness and capacity of the beam with corroded rebar in comparison to sound beam.

REFERENCES

- [1] X. Xue and H. Seki, "Influence of longitudinal bar corrosion on shear behavior of RC beams", *Journal of Advanced Concrete Technology*, vol. 8, no. 2, pp. 145-156, 2010.
- [2] S. F. U. Ahmed, M. Maalej, and H. Mihashi, "Cover cracking of reinforced concrete beams due to corrosion of steel", *ACI materials journal*, vol. 104, no. 2, pp. 153-161, 2007.
- [3] A. A. Almusallam, A. S. Al-Gahtani, and A. R. Aziz, "Effect of reinforcement corrosion on bond strength", *Construction and building materials*, vol. 10, no. 2, pp. 123-129, 1996.
- [4] G. Al-Sulaimani, M. Kaleemullah, and I. Basunbul, "Influence of corrosion and cracking on bond behavior and strength of reinforced concrete members", *Structural Journal*, vol. 87, no. 2, pp. 220-231, 1990.
- [5] F. Di Carlo, A. Meda, and Z. Rinaldi, "Structural performance of corroded RC beams", *Engineering Structures*, vol. 274, pp. 115117, 2023. <https://doi.org/10.1016/j.engstruct.2022.115117>
- [6] K. Toongoenthong and K. Maekawa, "Simulation of coupled corrosive product formation, migration into crack and propagation in reinforced concrete sections", *Journal of Advanced Concrete Technology*, vol. 3, no. 2, pp. 253-265, 2005.
- [7] T. K. Khoa, H. Nakamura, K. Kawamura, and M. Kunieda, "Analysis of crack propagation due to rebar corrosion using RBSM", *Cement and Concrete Composites*, vol. 33, no. 9, pp. 906-917, 2011.
- [8] J. Ožbolt, F. Oršanić, G. Balabanić, and M. Kušter, "Modeling damage in concrete caused by corrosion of reinforcement: coupled 3D FE model", *International journal of fracture*, vol. 178, pp. 233-244, 2012.
- [9] N. V. Chinh, B. Q. Hieu, and P. Lambert, "Experimental and numerical evaluation of the structural performance of corroded reinforced concrete beams under different corrosion schemes", *Structures*, vol. 45, pp. 2318-2331, 2022. <https://doi.org/10.1016/j.istruc.2022.10.043>
- [10] N. C. Luyen, H. Nakamura, T. Miura, and Y. Yamamoto, "Analysis of Corrosion-induced Crack Propagation of RC Members Modeling by Corrosion Expansion Pressure Around Beam Element", *Proceeding of JCI annual conventional*, vol. 39, no. 2, pp. 961-966, 2017.
- [11] N. C. Luyen, "Modelling the effect of rebar corrosion on RC structures using 3D-RBSM", *Journal of Water Resources and Environmental Engineering*, vol. 62, pp. 17-24, 2018.
- [12] Y. Yamamoto, H. Nakamura, I. Kuroda, and N. Furuya, "Analysis of compression failure of concrete by three-dimensional rigid body spring model", *Doboku Gakkai Ronbunshuu*, vol. 64, no. 4, pp. 612-630, 2008.
- [13] M. Suga, H. Nakamura, T. Higai, and S. Saito, "Effect of bond properties on the mechanical behavior of RC beam", *Proceedings of Japan Concrete Institute*, vol. 23, no. 3, pp. 295-300, 2001.